06,13

Reliability of MIS structures based on films of barium strontium titanate and hafnium oxide

© M.S. Afanasyev, D.A. Belorusov, D.A. Kiselev, V.A. Luzanov, G.V. Chucheva ¶

Fryazino Branch, Kotel'nikov Institute of Radio Engineering and Electronics, Russian Academy of Sciences, Fryazino, Moscow oblast, Russia

¶ E-mail: gvc@fireras.su

Received May 28, 2025
Revised October 1, 2025
Accepted October 2, 2025

Ferroelectric films of barium strontium titanate (BST) and hafnium oxide (HfO_2) were synthesized on silicon substrates by high-frequency sputtering and magnetron sputtering, respectively. The results of studies of the structural composition of BST and HfO_2 films and the electrophysical properties of metal-insulator-semiconductor (Ni-BST-Si) and (Ni-HfO_2-Si) MIS structures based on them are presented.

Keywords: ferroelectric films, barium strontium titanate (BST), hafnium oxide (HfO_2), metalinsulator-semiconductor (MIS) structures, electrophysical properties.

DOI: 10.61011/PSS.2025.10.62637.148-25

1. Introduction

Integration of ferroelectric materials with today's semiconductor technologies offer an opportunity of creating next generation hardware components of electronic devices based on the nonlinear physical effects [1–3]. However, there are a number of technical difficulties on the way of deploying such heterostructures. One of them is inability to use the existing equipment for testing the fabrication processes because of its possible contamination with the chemical elements of these compounds. Integration problems also include the need to significantly complicate the technological process and develop additional operations for it [3]. It should be stressed that during the formation of the ferroelectric films, mechanical stresses arise at the film-wafer interface. These stresses are related to the discrepancy between the parameters of the wafer and film crystal lattices and the difference in their thermal expansion coefficients, as a result of this, defects such as dislocations occur in the films, which lead to changes in the ferroelectric properties of heterostructures.

The purpose of the study is to determine the reliability of the fabricated MIS structures made of ferroelectric films of barium strontium titanate and hafnium oxide of various thicknesses.

2. Samples and experimental procedure

$Ba_{0.8}Sr_{0.2}TiO_3$ (BST) films were deposited on *n*-type (100) silicon wafers by the method of high-frequency (HF) sputtering of a stoichiometric target having the same composition under high oxygen pressure using „Plasma 50 SE" system. Conditions of BST films sputtering: 60 Pa oxygen pressure during sputtering, 10 mm distance between the target and the wafer, 630 °C temperature of the wafer. Under the given conditions the film growth rate was ≈ 6.0 nm/min.

HfO_2 films were formed on *n*-type (100) silicon wafers by magnetron sputtering of a ceramic target having the same composition. Basic parameters of film sputtering: target-wafer distance — 50 mm, diameter of the sputtered target — 70 mm, operating pressure in the chamber $3 \cdot 10^{-3}$ Torr. The radiation heating of the wafer in the process of sputtering provided sufficient surface mobility of the deposited particles to form the oxide.

To investigate the electrophysical properties of the obtained films Ni-BST-Si and Ni-HfO_2-Si structures were formed. For this, the formed BST and HfO_2 films were coated with an electrode deposited by the method of an e-beam sputtering through the shadow mask. Electrode material — nickel, area of $2.7 \cdot 10^{-4}$ cm^2, thickness 0.1 μm. Sputtering parameters: residual pressure in the chamber — 10^{-4} Pa, structure temperature — 70 ± 5 °C, sputtering rate — 2.0 ± 0.2 Å/s.

The crystalline structure of the films was investigated by the X-ray diffraction analysis using DRON-3 automated double-crystal Bragg–Brentano diffractometer. An X-ray tube with a copper anode (wavelength 0.1541 nm) was used as the radiation source. A quartz monochromator was used to differentiate the $K\alpha_1$ line in the spectrum. Capacitance-voltage (C-V) curves of MIS structures were measured by an automated experimental setup [4] using a precision meter LCR E4980A (Agilent).

Two types of MIS structures Ni-BST-Si and Ni-HfO_2-Si with the thicknesses of BST and HfO_2 $h = 20$ films 100 and 150 nm, respectively, were fabricated for the study.

3. Results and discussion

3.1. Structural studies of MIS structures

Figure 1 illustrates the diffraction patterns of the fabricated BST and HfO_2 films with a thickness of 150 nm.

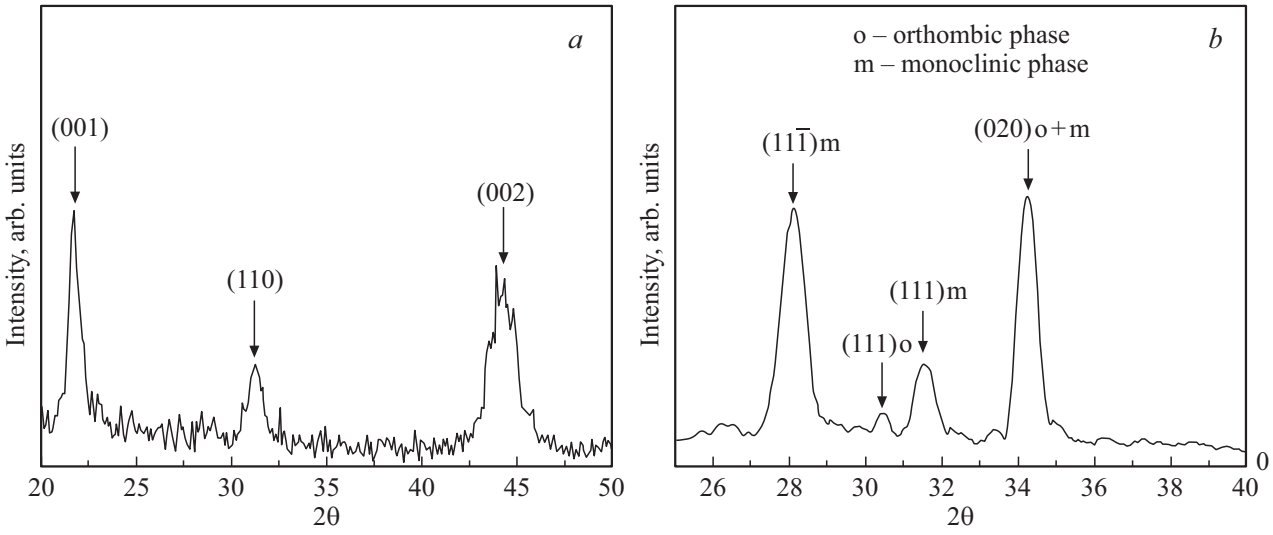

Figure 1. X-ray diffraction patterns of 150 nm thick films. BST/Si (*a*) and HfO_2/Si (*b*).

Both diffraction patterns show peaks from different lattice planes of BST and HfO_2 films. This indicates that the films are polycrystalline without signs of predominant orientation. At the same time, reflections from both the monoclinic and polar orthorhombic phases can be seen on the diffraction patterns from HfO_2 film, which is believed to impart ferroelectric properties to HfO_2. An estimate of the size of coherent scattering regions (CSR) using Debye-Scherrer method showed that for a BST film, the average CSR size was about 5 nm, for HfO_2 — 10 nm.

Earlier in [5] we obtained numerical values of surface roughness and average crystallites size for the studied films, which also demonstrate large lateral crystallite values for HfO_2 films compared with BST while having the same thicknesses, which correlates with X-ray diffraction analysis data.

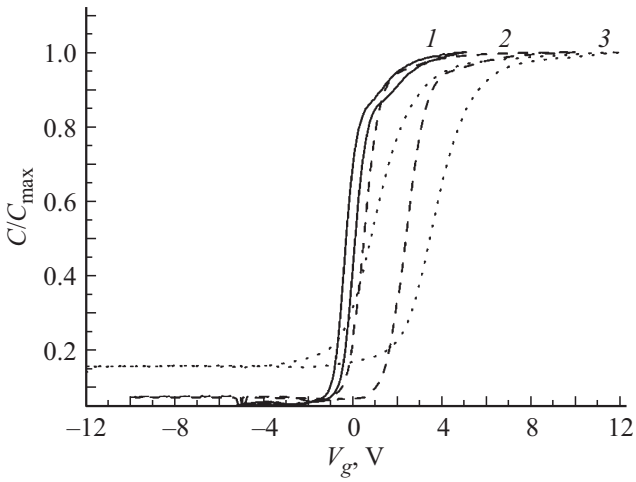

Figure 2. C-V curves of Ni-BST-Si structures with the following thicknesses of BST films: *1* — 20 nm, *2* — 100 nm, *3* — 150 nm.

3.2. Electrophysical properties of MIS structures

3.2.1. Electrophysical properties of Ni-BST-Si structures

Figure 2 shows capacitance-voltage curves of Ni-BST-Si MIS structures with the thickness of BST film $h = 20$, 120 and 150 nm. The measurements were carried out at room temperature and a frequency of 1 MHz with a vertical sweep of 100 mV/sec. The dependencies of capacitance on bias voltage had a hysteresis loop shape. The voltage values were selected based on obtaining the largest width of the hysteresis loop without damaging the MIS structures. Bias voltage (V_g) during measurement ranged: from -5 to 5 V, from -10 to 10 V and from -12 to 12 V and vice versa for the MIS structures with thickness of $h = 20$, 100 and 150 nm, respectively. Due to the difference in thickness of the films, the capacity values of C/C_{max} were normalized to compare the obtained results.

With the decrease in BST film thickness, it resulted in higher maximum of capacitance $C_{max} = 139.11$, 130.24, 33.94 pF and reduced width of the hysteresis loop 0.43, 1.91, 2.64 V, and $h = 20$, 100, and 150 nm respectively. It shall be noted that a decrease in the film thickness also led to a shift in the center of the C-V curve symmetry towards the negative stresses region. The shift is apparently related to a change in the concentration of the built-in charge at the ferroelectric/wafer interface.

Figure 3 illustrates the frequency behavior of capacitance (C) and dielectric loss angle tangent ($\mathrm{tg}\,\delta$) of Ni-BST-Si MIS structures, measured at room temperature and permanent bias voltage of $V_g = +5$, $+10$, $+12$ V for BST film $h = 20$, 100 and 150 nm, respectively.

Capacitance versus frequency change pattern is identical for the MIS structures. When the frequency was increased, the change in the capacitance did not exceed 10 %. The dependence $\mathrm{tg}\,\delta(f)$ had the form of a linear function. As the thickness of the BST film declined, the steepness of the

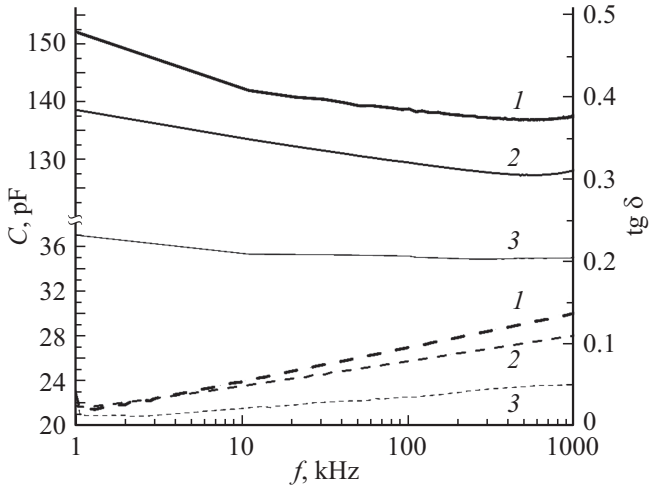

Figure 3. C (solid lines) and $\mathrm{tg}\,\delta$ (dashed lines) versus frequency (f) of Ni-BST-Si structures with a thickness of BST film: *1* — 20 nm, *2* — 100 nm, *3* — 150 nm.

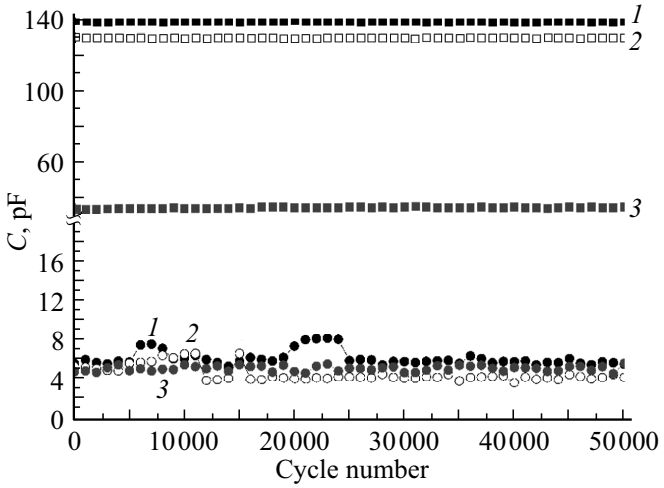

Figure 4. $C_{\max}$ (squares) and $C_{\min}$ (circles) versus number of the switching cycles for Ni-BST-Si structures with BST film thickness: *1* — 20 nm, *2* — 100 nm, *3* — 150 nm.

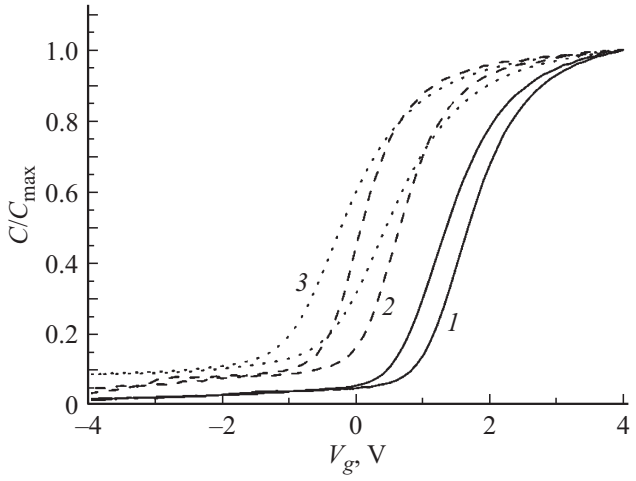

Figure 5. The capacitance-voltage curves of Ni-HfO_2-Si structures with thickness of HfO_2 films: *1* — 20 nm, *2* — 100 nm, *3* — 150 nm.

characteristics $\mathrm{tg}\,\delta(f)$ increased. A decrease in the thickness of the ferroelectric film led to higher values of $\mathrm{tg}\,\delta$.

Figure 4 shows the dependence of the maximum and minimum capacitance on the number of switching cycles of the MIS structures obtained at room temperature at a frequency of 1 MHz. V_g was cyclically applied to the samples, corresponding to the values of the maximum and minimum C (see Figure 2). The delay time at each V_g was 0.5 s. Thus, one switching cycle was made in 1 s. A test was conducted with $5 \cdot 10^4$ number of switching.

It is shown that during $5 \cdot 10^4$ switching, the change in maximum and minimum capacitance, as well as the value of the capacitance ratio ($C_{\max}/C_{\min}$) did not exceed 5 %.

3.2.2. Electrophysical properties of Ni-HfO_2-Si structures

The capacitance-voltage curves of Ni-HfO_2-Si structures at room temperature and a frequency of 1 MHz are shown in Figure 5. The range of bias voltage V_g was from −4 to 4 V.

As in the case of Ni-BST-Si structures, a lower film thickness led to a decrease in the steepness and width of the hysteresis loop, however, the opposite shift of the hysteresis loop center of symmetry towards positive stresses was noticeable.

Capacitance maximum was 148.46 pF at $h = 20$ nm, 75.36 pF at 100 nm and 50.35 pF at 150 nm, and hysteresis loops widths — 0.32 V at $h = 20$ nm, 0.57 V at 100 nm and 0.68 V at 150 nm.

The change pattern in the frequency dependence of the capacitance on the layer thickness is similar to Ni-BST-Si structures, however, the value of the capacitance does not change by more than 5 %. The dependence of $\mathrm{tg}\,\delta(f)$ for samples with $h = 150$ and 100 nm is more stable in terms of frequency compared to structures with $h = 20$ nm, where $\mathrm{tg}\,\delta$ drastically changes within the frequency range 1 —

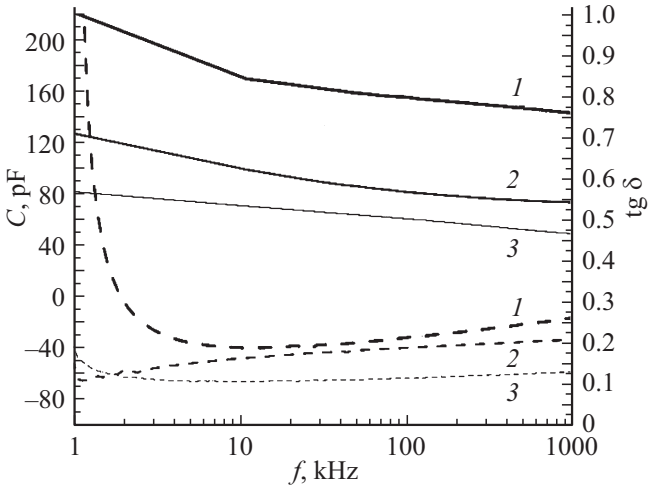

Figure 6. C (solid lines) and $\mathrm{tg}\,\delta$ (dashed lines) versus frequency f of Ni-HfO_2-Si structures with the film thickness HfO_2: *1* — 20 nm, *2* — 100 nm, *3* — 150 nm.

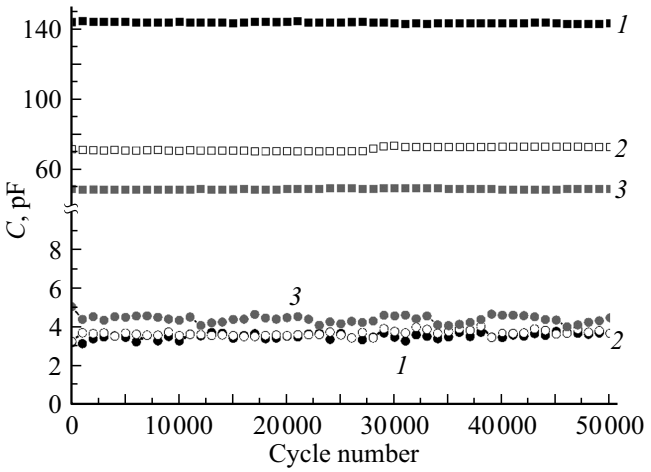

Figure 7. C_{max} (squares) and C_{min} (circles) versus number of switching cycles for Ni-HfO_2-Si structures with the thickness of HfO film$_2$: *1* — 20 nm, *2* — 100 nm, *3* — 150 nm.

10 kHz. Compared to Ni-BST-Si structures the values tg δ for Ni-HfO_2-Si are 1.5 times higher (Figure 6).

Figure 7 shows the dependences of the maximum and minimum capacitance on the number of switching cycles of MIS structures obtained at room temperature at a frequency of 1 MHz. The change in maximum and minimum capacitance, as well as the value of the capacitances ratio (C_{max}/C_{min}) during $5 \cdot 10^4$ the number of switching didn't exceed 3 %.

4. Conclusion

The effect of the thickness of BST and HfO_2 films formed on silicon wafers by HF sputtering and magnetron sputtering, respectively, on the electrophysical properties of the related MIS structures. The MIS structures Ni-BST-Si, in general, are found to have higher breakdown voltages compared to Ni-HfO_2-Si. The pattern of MIS structures properties variation with the change of the thickness of BST and HfO_2 layers is found to be identical. A decrease in the film's thickness leads to a reduction in the width of the capacitance-voltage hysteresis loops, which indicates a lower degree of the film's crystallinity, as well as a shift in the loops' center of symmetry, which is most likely due to a change in the concentration of the built-in charge at the ferroelectric/wafer interface. Cyclic measurements have demonstrated sufficient stability of the MIS structures. After $5 \cdot 10^4$ switchings the change in the values of (C_{max}/C_{min}) was no higher than 5 %. At the same time, reliability of the MIS structures is not compromised with a decrease in the films thickness.

Funding

This study was supported by the Russian Science Foundation, grant № 23-49-10014, https://rscf.ru/project/23-49-10014/

Conflict of interest

The authors declare that they have no conflict of interest.

References

[1] Fizika segnetoelektrikov: sovremennyi vzglyad: uchebnoye posobiye / Pod red. K.M. Rabe [et al.]. 3-e izd. (el.) Laboratoriya znanii, M. (2015). 443 p. (in Russian).
[2] D.A. Abdullaev, R.A. Milovanov, R.L. Volkov, N.I. Borgardt, A.N. Lantsev, K.A. Vorotilov, A.S. Sigov. Ross. Tekhnol. Zh., **8**, *5*, 44 (2020).
[3] K.A. Vorotilov, V.M. Mukhortov, A.S. Sigov. Integrirovannye segnetoelektricheskie ustroystva /Pod red. A.S. Sigov Energoatomizdat, M., (2011). 175 p. (in Russian).
[4] E.I. Goldman, A.G. Zhdan, G.V. Chucheva. Instruments and experimental techniques, **40**, *6*, 841 (1997).
[5] M.S. Afanasyev, D.A. Belousov, D.A. Kiselev, V.A. Luzanov, G.V. Chucheva. RENSIT: Radioelektronika. Nanosistemy. Informatsionnyie tekhnolgii. **16**, *7*, 867 (2024).

Translated by T.Zorina